The Journal of Chemical Physics

Band-like transport in "green" quantum dot films: The effect of composition and stoichiometry

Cite as: J. Chem. Phys. **156**, 104704 (2022); https://doi.org/10.1063/5.0078375
Submitted: 12 November 2021 • Accepted: 15 February 2022 • Accepted Manuscript Online: 17 February 2022 • Published Online: 09 March 2022

Panagiotis Rodosthenous, E. S. Skibinsky-Gitlin, Salvador Rodríguez-Bolívar, et al.

The Journal of Chemical Physics ARTICLE scitation.org/journal/jcp

Band-like transport in "green" quantum dot films: The effect of composition and stoichiometry

Cite as: J. Chem. Phys. 156, 104704 (2022); doi: 10.1063/5.0078375
Submitted: 12 November 2021 • Accepted: 15 February 2022 •
Published Online: 9 March 2022

Panagiotis Rodosthenous,[1] E. S. Skibinsky-Gitlin,[2] Salvador Rodríguez-Bolívar,[2,3] Marco Califano,[1,4] and Francisco M. Gómez-Campos[2,3,a)]

AFFILIATIONS

[1] Pollard Institute, School of Electronic and Electrical Engineering, University of Leeds, Leeds LS2 9JT, United Kingdom
[2] Departamento de Electrónica y Tecnología de Computadores, Facultad de Ciencias, Universidad de Granada, 18071 Granada, Spain
[3] CITIC-UGR, C/ Periodista Rafael Gómez Montero, número 2, Granada, Spain
[4] Bragg Centre for Materials Research, University of Leeds, Leeds LS2 9JT, United Kingdom

Note: This paper is part of the JCP Special Topic on Transport of Charge and Energy in Low-Dimensional Materials.
[a)] **Author to whom correspondence should be addressed:** fmgomez@ugr.es

ABSTRACT

Two-dimensional quantum dot (QD) arrays are considered as promising candidates for a wide range of applications that heavily rely on their transport properties. Existing QD films, however, are mainly made of either toxic or heavy-metal-based materials, limiting their applications and the commercialization of devices. In this theoretical study, we provide a detailed analysis of the transport properties of "green" colloidal QD films (In-based and Ga-based), identifying possible alternatives to their currently used toxic counterparts. We show how changing the composition, stoichiometry, and the distance between the QDs in the array affects the resulting carrier mobility for different operating temperatures. We find that InAs QD films exhibit high carrier mobilities, even higher compared to previously modeled CdSe (zb) QD films. We also provide the first insights into the transport properties of properly passivated InP and GaSb QD films and envisage how realistic systems could benefit from those properties. Ideally passivated InP QD films can exhibit mobilities an order of magnitude larger compared to what is presently achievable experimentally, which show the smallest variation with (i) increasing temperature when the QDs in the array are very close and (ii) an increasing interdot distance at low operating temperatures (70 K), among the materials considered here, making InP a potentially ideal replacement for PbS. Finally, we show that by engineering the QD stoichiometry, it is possible to enhance the film's transport properties, paving the way for the synthesis of higher performance devices.

INTRODUCTION

The unique size-tunable optical properties of semiconductor quantum dots (QDs) make these systems ideal candidates for a wide range of applications.[1,2] In addition, the combination of strong interdot coupling along with the assembly of QDs in arrays can create novel materials that take advantage of such properties and the high carrier mobilities of the bulk.[3] However, the mechanisms involved in carrier transport in these materials are still debated. One of the approaches is to model carrier transport by hopping, where the electron "hops" from a localized quantum dot state to another in the array.[4] Another approach is to model carrier transport by band-like mechanisms: the array regimentation leads to the rise of a band structure from the isolated QD states (miniband structure due to the narrower band widths).[5,6] In general, it is accepted that the signature of band-like transport is the decrease in carrier mobility with temperature, although this behavior could also be reproduced in hopping transport in a reduced temperature range.[6] However, the experimental trend is toward achieving periodic QD regimentation and reducing the interdot distances by reducing the size of the ligands. In this regime, the eigenstates of the individual quantum dots are expected to exhibit strong coupling, leading to band formation. Aiming to model transport in such systems, we will then apply a band-like approach.

A particular case of QD array is the colloidal QD (CQD) film, a two-dimensional array that, also due to its cost-effective synthesis,[7] finds applications in many fields, such as photovoltaics, optoelectronics, LEDs, and transistors.[8–11] The best characterized and more commonly used QD films are made of Cd and Pb chalcogenides, whose heavy metal content, unfortunately, makes them toxic and limits their commercialization.[12] It is, therefore, crucial to find suitable, non-toxic, replacement materials that exhibit similar properties for a specific application without the environmental cost. We previously calculated the mobility of zinc blende CdSe and InAs QD films using a simple approach[13] and found that they are similar. This similarity in the transport properties of two very different materials is surprising and seems to suggest that the intrinsic nature of the QD in this case is unimportant. Using a more sophisticated methodology here, we pursue this issue further, extending our investigation to a wider range of "green" III–V materials, with the aim of identifying possible alternatives to both Cd- and Pb-based materials for efficient transport in 2D QD arrays.

METHOD

We study carrier transport in QD films consisting of same-sized QDs two-dimensionally periodically distributed. In our calculations, we assume that the electrons are scattered by fluctuations in the dot size,[14] due to the presence of dots with a smaller diameter compared to the periodic ones with radius R–δR acting as scattering centers (impurity dots). Indeed, owing to the nature of these systems, phonon scattering, which dominates in the bulk, is negligible in 2D QD arrays.[6] To investigate the effect of different anions, we considered In-based materials (InP, InAs, and InSb), and we then studied the effect of changing the cation from InSb to GaSb. Our periodic dots have a total of 275 atoms while the impurities have 199 atoms and the radius of the QDs differs for each material due to the different lattice constant. The exact same dots were used for all materials considered here, but changing the atomic types accordingly.

Our individual QDs were generated by starting from a central atom and adding atomic layers up to a specific cut-off radius. The QD surfaces were terminated using ideal passivants (eliminating any surface states).[15] The single-particle energies (red dashed lines in Fig. 1) and wave functions of the isolated dots were obtained by solving the Schrödinger equation (including spin–orbit coupling), using the state-of-the-art semiempirical pseudopotential method.[16] A periodic array is modeled by placing quantum dots in a square lattice. The quantum dots were separated by the interdot distance (d), defined as the distance between the surface atoms of neighboring QDs in the array, measured in bond lengths (b.l.). In our calculation, we assume 1 b.l. as the minimum distance between two QDs. Two different stoichiometries were considered in each case (cation-centered and anion-centered leading to anion-rich and cation-rich surfaces, respectively). A 1% density of impurities was assumed as a realistic value in accordance with experimental samples.[17]

We solved the Schrödinger equation of the QD film by means of the tight-binding model using a basis consisting of seven or eight conduction band eigenstates of the QD, depending on the material. This yields the electronic structure of the system, i.e., the QD film miniband structure, as shown in Fig. 1, where the reduced miniband widths, compared to bulk, imply increased values for the corresponding effective masses. In Fig. 1, all minibands are shifted to lower energies, compared to the positions of the isolated QD levels from which they originate (red dashed lines in the figure), due to the interdot interactions in the film. Indeed, according to the tight-binding approach,[18] in a simple single-band case, the lowest energy miniband exhibits a shift from the isolated dot conduction-band minimum (CBM) energy approximately equal to the integral $\int \phi^*_{CBM}(\vec{r}) \sum_{\vec{R}_n} V(\vec{r}-\vec{R}_n) \phi_{CBM}(\vec{r}) d\vec{r}$, where $\phi_{CBM}(\vec{r})$ is the CBM wave function of the isolated dot, $V(\vec{r}-\vec{R}_n)$ is the potential of the neighboring dot, and the summation runs over the number of nearest neighbors (four in a square lattice). We find that GaSb QD films yield the largest value of this integral (−91 meV per neighbor), hence exhibit the largest shift, followed by InP (−62 meV per neighbor), InSb (−48.7 meV per neighbor), and InAs QD films (−46 meV per neighbor), reflecting the shifts shown in Fig. 1.

In the next step, the semiclassical transport model described in Ref. 6 is implemented. Fermi's Golden Rule is used to compute the electron scattering rates. The scattering mechanism is elastic, and, therefore, the initial and final states have the same energy. The scattering rate for an electron in the lowest energy miniband to scatter from state i to state f is obtained as

$$\Gamma_{i,f} = \frac{2\pi\nu}{Q_s \hbar \Delta E} |\langle f|\Delta V|i\rangle|^2, \tag{1}$$

where ν is the impurity ratio in the sample, Q_s is the number of states sampled in the reciprocal space, $\hbar$ is the reduced Planck constant, ΔE is the energy interval in which scattering is considered elastic (due to numerical implementation, transitions between states with energies within the energy interval are considered to conserve energy), f and i stand for the final and initial eigenstate wave functions, and ΔV is the perturbation to the periodic potential of the array, i.e., the difference between the potentials of the periodic and the impurity dot. This difference is mainly observed close to the QD surface because the impurities are obtained by removing atoms from the surface of the periodic dot. As a consequence, the difference between periodic and impurity QD potentials, together with the behavior of the wave functions of the initial and final states, is crucial to determine the flight times between scatterings. The average flight time has been calculated by averaging the flight times of a sampling of 51 × 51 initial states in the Brillouin zone. The error corresponds to the flight time's standard deviation.

Once $\Gamma_{i,f}$ are obtained for each pair of states in the miniband conserving energy, mobility is obtained using the formalism presented in Ref. 6. For a given electric field, the average electron velocity depends on the direction of application because of the anisotropy of the QD film. Two eigenvalues of the mobility tensor are presented throughout this study for each QD film, corresponding to two perpendicular directions in the 2D plane of the film. The Fermi energy (E_F) was placed at the bottom of the lowermost conduction miniband. This can be achieved by either a moderate photodoping in the system or impurity doping in the neighboring regions. An electric field of 1×10^3 V/m was used, low enough to be in the ohmic regime and high enough to guarantee the numerical stability in the calculation.

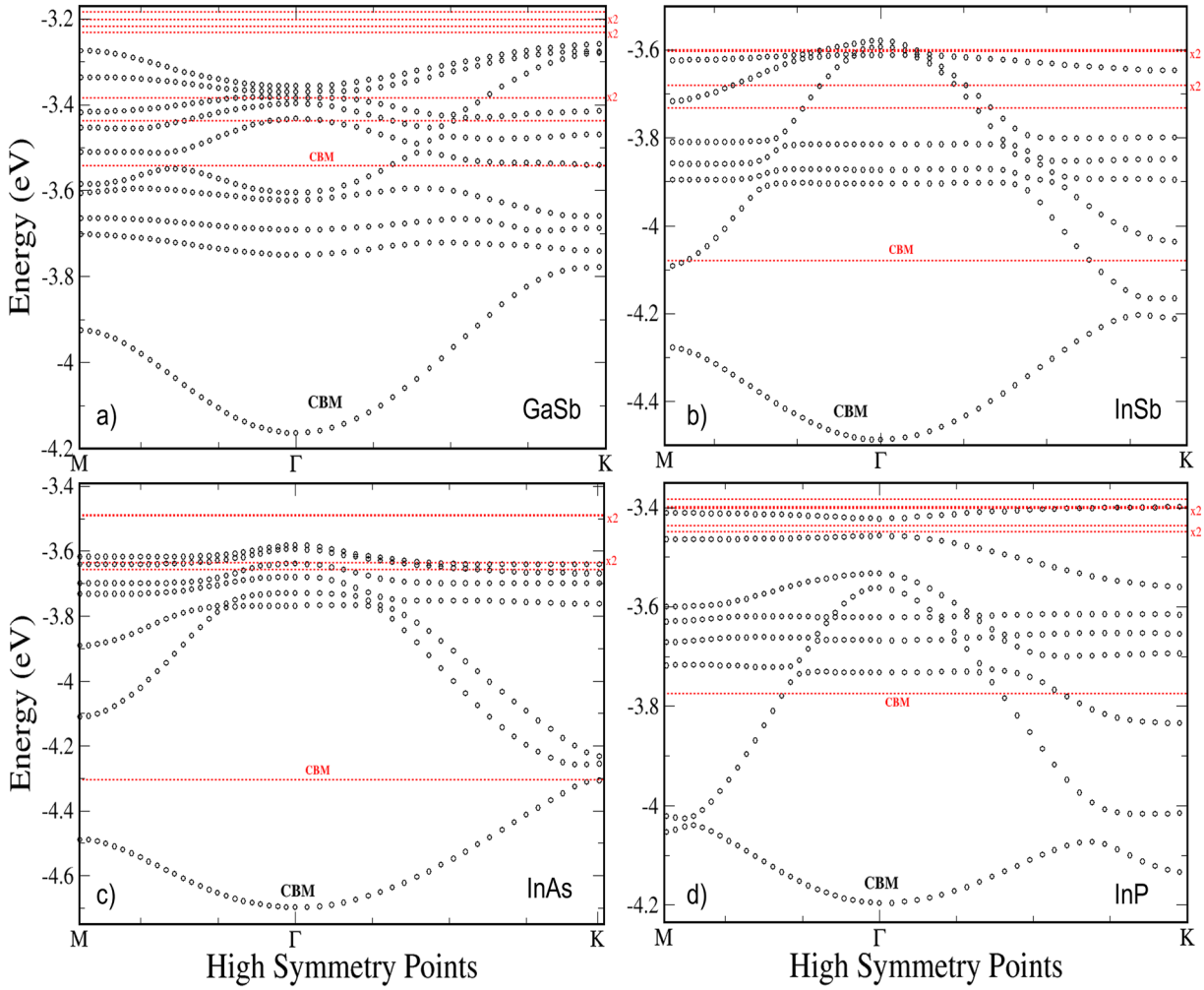

FIG. 1. Conduction miniband structure for (a) GaSb, (b) InSb, (c) InAs, and (d) InP QD films in the reciprocal space (black dots), together with the corresponding CB eigenvalues of the isolated dots (red dashed lines).The calculated energies are relative to vacuum.

In-BASED QD FILMS

Isolated In-based QDs have been proposed as promising candidates for replacing their toxic counterparts (e.g., CdSe, PbSe, PbS, etc.). This work aims at investigating whether this replacement is also viable in the case of 2D arrays.

The mobility of films of InAs CQDs is calculated for temperatures ranging between 50 and 350 K (corresponding to a realistic range for device operation), and our results are compared with the available experimental data. Figure 2 illustrates the mobility dependence on temperature for four different interdot separations for this material. The specific values for d are related to the sampling of the bulk crystal unit cell in grid points. The values of d correspond to increments in the QD separations of two grid points. Although the carrier mobility decreases with increasing temperature, as expected in band-like transport, this decrease is much less dramatic than what is found in bulk semiconductors, in agreement with experimental observation,[3,17] due to the different scattering mechanism limiting transport in the two systems. The decay rate becomes larger with increasing d: for d = 1 b.l., the decay is ~ linear, while for larger d, it becomes more exponential. Additionally, as d is increased, the mobility value for a given temperature is reduced due to the weaker wave function overlap between neighboring QDs. In Fig. 3, we investigate the variation of mobility with increasing separation for two different temperatures (one for device operation at low temperatures and one for operation at higher temperatures). The mobility for an interdot separation of 1 bond length is not affected much by the change in temperature, however, placing the QDs in the array even further causes the mobility to drop with much faster rates. We find that this decay is nearly exponential. The origins of this behavior can be attributed to the exponential dependence on d of the wave function overlap between neighbor quantum dots, which determines the miniband width (defined as the difference between the lowermost energy point and the highest energy point of the miniband): the

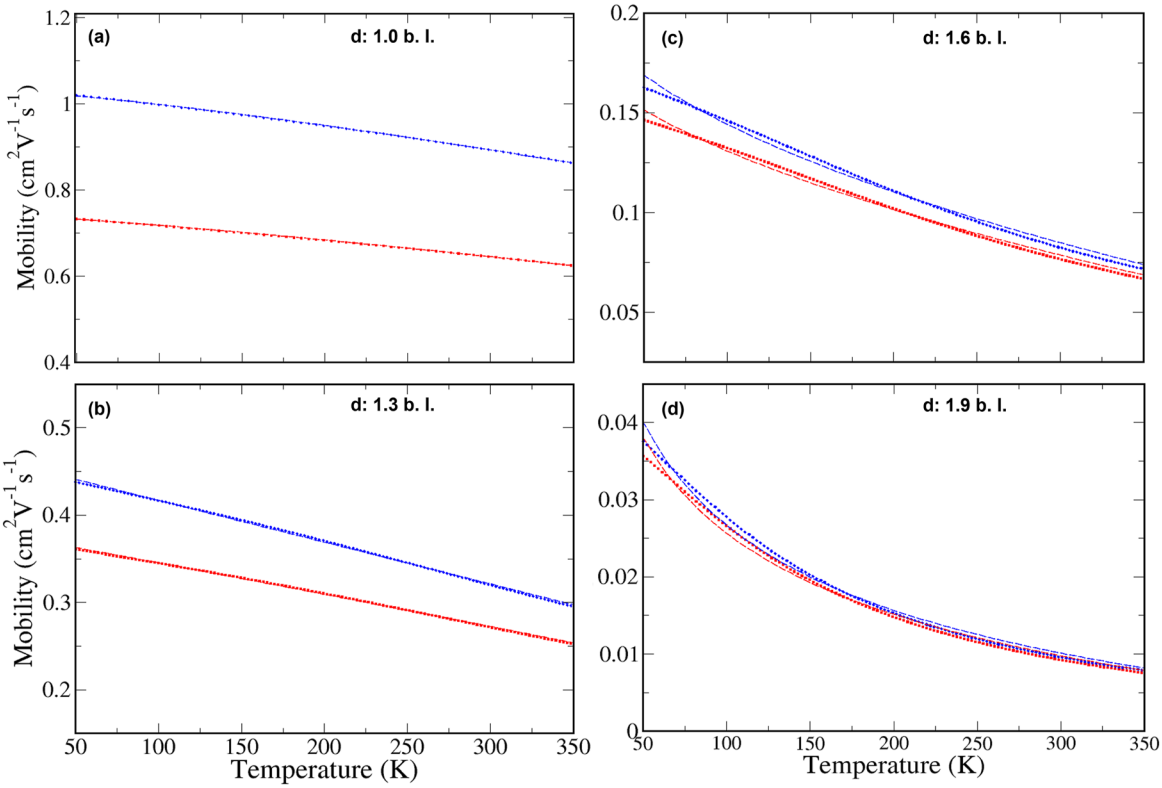

FIG. 2. Electron mobility as a function of temperature for InAs QDs, where the QDs are separated by (a) 1, (b) 1.3, (c) 1.6, and (d) 1.9 b.l. The blue circles and red squares represent the two eigenvalues of the mobility tensor. The blue and red lines are the respective fittings.

larger the overlap, the wider the miniband. Wide minibands lead to smaller effective masses and, therefore, higher mobilities in general. Therefore, increasing the interdot distance would result in an exponential increase in the effective mass and, therefore, an exponential decrease in mobilities (see Fig. S10 in the supplementary material).

For higher temperatures, this decay rate is slightly faster compared to lower temperatures. It was previously shown experimentally[19] that by using InAs QDs capped with molecular metal chalcogenide ligands, the electron mobility is nearly 1 order of magnitude larger than what we find here. This is attributed to the fact that those

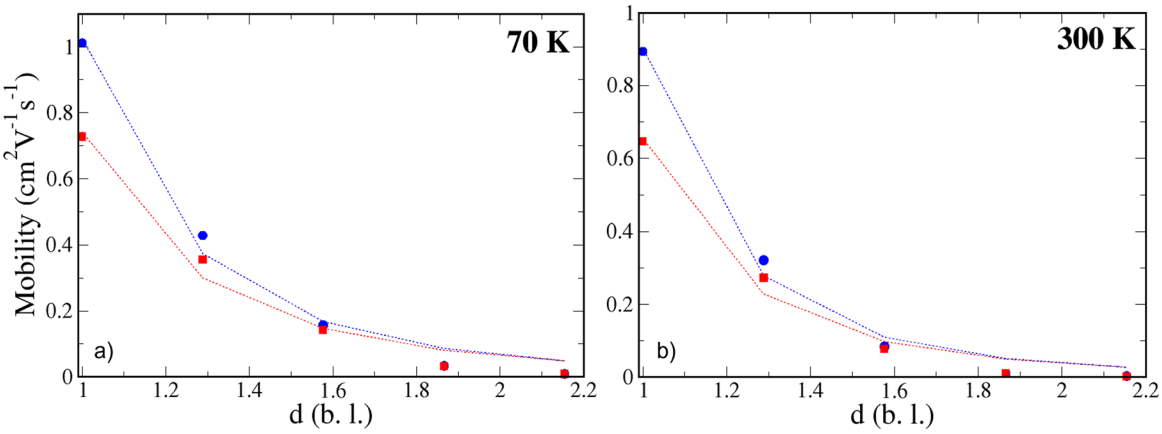

FIG. 3. Mobility as a function of increasing interdot separation for (a) 70 and (b) 300 K for InAs QD films. The blue circles and red squares represent the mobility tensor eigenvalues. The dashed lines represent a theoretical fitting to our findings.

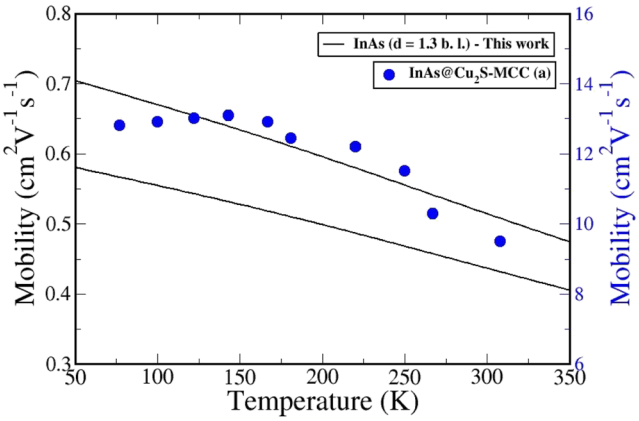

FIG. 4. Mobility as a function of temperature: comparison with the experiment: (a) Ref. 19. Our mobility eigenvalues (left y axis) are shown as black lines while the experimental data (right y axis) are presented with blue dots.

ligands act as a "bridging" mechanism for the QDs in the array. The same study emphasizes the importance of the surface termination of QDs when it comes to the determination of their transport properties: different capping agents can yield different interdot coupling.

Their experimental trend of mobility vs temperature is in qualitative agreement with our results as can be seen in Fig. 4(a), where the range of the y-axis for the two cases is different. (The right-hand y-axis is obtained by multiplying the y-axis on the left by a factor of 20.) A similar decay rate for the mobility decrease with temperature was also observed in InAs films[20] (i.e., in 2D InAs, as opposed to 2D arrays of InAs QDs), where band-like transport is expected. Mobilities with similar values (1.1 $cm^2\ V^{-1}\ s^{-1}$) to those we find in InAs QD films were recently measured in $MAPbI_3$ thin films by Sanehira *et al.*[21] In addition, they synthesized $CsPbI_3$, FAI–$CsPbI_3$, PbS, and PbSe QD films with mobilities of 0.2, 0.5, 0.04, and 0.08 $cm^2\ V^{-1}\ s^{-1}$, respectively, at room temperature, which are all lower compared to our InAs QD films. These results suggest that (i) InAs QD films could be good candidates to replace Pb-based QD films, at least from the point of view of their mobility and (ii) as our transport results reproduce observed trends, the carrier dynamics in real samples could be close to that modeled in our approach.

From the point of view of their mobility, InAs QD films can also be considered as potential replacements for Cd-based QD films. Indeed, the mobility for zinc blende CdSe (zb) QD films of identical size to the QDs considered here was predicted[13] to be 1 $cm^2\ V^{-1}\ s^{-1}$ at room temperature and with an interdot separation of 1 bond length, which is similar to the mobility of InAs QD films in this work, and it is in agreement with the experiment.[3,22]

Keeping the cation the same and replacing As with P, we find that the value of the mobility for all interdot separations and all temperatures is reduced (see Fig. S1 in the supplementary material). The decay rate with increasing d is similar to InAs (see Fig. S2 in the supplementary material). The mobility reduces gradually from ~0.65 to ~0.01 $cm^2\ V^{-1}\ s^{-1}$ with d increasing from 1 to 2.2 b.l., at room temperature.

In general, InP QDs commonly synthesized in the lab suffer from poor surface quality and surface passivation problems, similarly to CdS QDs.[23] Experimental results on InP QD films were recently reported[24] showing that films based on InP QDs exhibit surface traps problems, leading to weak emission and reduced electron mobility (0.035 $cm^2\ V^{-1}\ s^{-1}$). It was found that the addition of Zn during the synthesis process leads to the elimination of those traps, forming InZnP QD films with even lower mobility (as the Zn:In ratio is increased, the mobility is reduced). The observed mobility for InP QD films is lower compared to PbSe[25] (~0.1 – 1 $cm^2\ V^{-1}\ s^{-1}$) and it is similar to PbS[26] (~10^{-3} – 10^{-2} $cm^2\ V^{-1}\ s^{-1}$) QD films, but an order of magnitude lower compared to CdSe[27] QD films with similar treatments. Our findings show that InP QD films, when passivated properly,[28] can exhibit carrier mobilities of the order of 0.5–0.7 $cm^2\ V^{-1}\ s^{-1}$ at room temperature. Recently, Crisp *et al.*[29] synthesized InP QD films deposited with crystalline ZnO films, yielding carrier mobilities of ~4 $cm^2\ V^{-1}\ s^{-1}$ and charge separation between QDs and ZnO. Their films were, however, infilled and overcoated by ZnO films, which, acting as an electron extraction layer, greatly improved both the carrier mobility and their lifetime. In another experiment,[19] a ~96% decrease in mobility (from 1.9 to 0.07 $cm^2\ V^{-1}\ s^{-1}$), attributed to surface traps and non-ideal passivation was observed when replacing As with P. We show that an ~60% decrease is expected even in the case of ideally passivated QDs. The sizes of their samples were (4.8 ± 0.5) nm for InAs and (3.8 ± 0.4) nm for InP QDs, about three times larger compared to our QDs. QDs with a larger size in the array lead to lower mobility values.

InSb has the highest carrier mobility in the bulk among the rest of the In-based materials considered here,[30] however, the electron mobility at nanoscale is similar to the mobility found in InAs QDs, for the same interdot separation.[31] The variation in the mobility with increasing temperature and interdot separation for InSb films is presented in Figs. S3 and S4 (supplementary material). Specifically, we calculate a mobility of ~0.82 $cm^2V^{-1}s^{-1}$ at T = 300 K. We see that InSb lies between InAs and InP in the hierarchy of higher-to-lower mobility. The behavior of InSb QD films is very similar to the corresponding InAs films described above. Unfortunately, as, to the best of our knowledge, there are no existing experimental or theoretical studies on the transport properties of InSb QD films, we could find no benchmark with which to compare our results.

Ga-BASED QD FILMS

Having considered In-based QD films with different anions, we then proceeded to replace the cation, obtaining GaSb, a green nanomaterial studied before.[32] Interestingly, we find that the mobility becomes about three times smaller compared to InSb. Specifically, the mobility drops from ~0.84 to ~0.28 $cm^2\ V^{-1}\ s^{-1}$ for d = 1 b.l. at T = 300 K, as shown in Fig. S5 (supplementary material). We also find that the two eigenvalues for the calculated mobility for the smallest separation considered here are closer, compared to the other materials. This is shown in Fig. S6 (supplementary material) and it is attributed to the isotropic nature of GaSb lowermost miniband structure around gamma, as illustrated in the 2D miniband representation of Fig. 1(a) for d = 1 b.l. and in a top-view miniband representation of Fig. S7 (supplementary material). The latter shows clearly that the lowermost miniband of GaSb QD films for d = 1 b.l. has an almost perfect circular shape around the miniband minimum,

while the InP miniband is the most anisotropic. The miniband curvature around the minimum, where most of the carriers are found, influences the mobility eigenvalues. We find that the change in the cation atom leads to a smaller wave function overlap between neighboring QDs compared to the In-based materials, yielding the lowest average flight times of $(5.14 \pm 2.06) \times 10^{-16}$ s (see Table S1 in the supplementary material). These flight times are much shorter than the flight times originating from phonon scattering in bulk semiconductors, reflecting both the different scattering mechanisms at play in QD films (impurity) and the magnitude of the resulting mobilities. Indeed, rates of the order of 10^{16} s^{-1} were recently calculated[33] for elastic alloy disorder scattering (which is similar in nature to impurity scattering) in III–V superlattices.

Comparing the miniband representations for each material, it is evident that In-based QD films have a different behavior compared to GaSb. To fully understand the origins of this difference, we analyzed the perturbation ΔV of the QD potential due to impurities in the film [see Eq. (1)]. We found that the perturbation in GaSb has different features compared to In-based materials, resulting in different typical values of Γ [in Eq. (1)], the transition rate between the initial (i) and final (f) state after scattering. The calculation of the mobility includes contributions from both the lowermost miniband width (that is linked to the effective mass) and the flight time of the carriers during their scattering [that is linked to the typical values of Γ in Eq. (1)]. We find that GaSb QD films, even though they have the highest miniband width for nearly all the separations considered here, exhibit the lowest average flight times (see Fig. 5). In order to achieve high carrier mobilities, a combination of both large miniband widths and high flight times is required. For In-based QD films, the flight times are similar, therefore, it is the miniband width that determines the mobility: films of InAs QDs have the largest miniband width among the In-based materials, thus, the highest mobility followed by InSb and InP, reflecting the order of decreasing miniband width. On the other hand, GaSb QD films have a miniband width comparable with InAs QD films and larger than InSb QD films at d = 1 b.l., however, the flight times for this material are ~4 times lower compared to InSb QD films, yielding the smallest mobility of all (around three times smaller compared to InSb QD films).

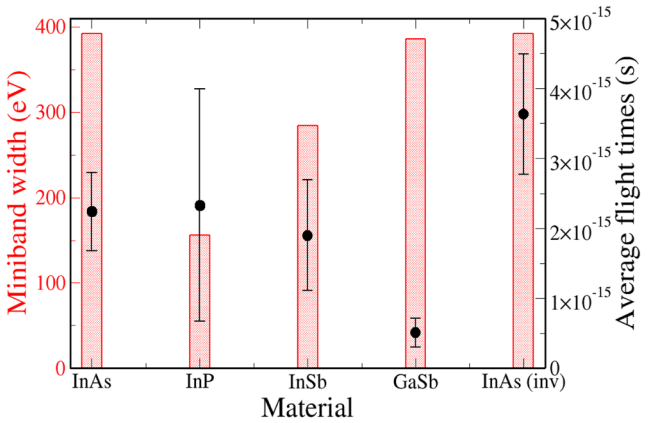

FIG. 5. Lowermost miniband width and corresponding average flight times for d = 1 b.l., for each material. The average flight time has been calculated by averaging the flight times of a sampling of 51 × 51 initial states in the Brillouin zone. The error interval corresponds to the flight time's standard deviation.

As an interdot separation of 1 b.l. may be difficult to achieve in some experimental films, we calculated the variation in the miniband width with increasing d, shown in Fig. S10 (supplementary material). The miniband width decreases with increasing d due to the weaker wave function overlap between the QDs. The same is true for the flight times. Consequently, mobilities calculated here for d = 1 b.l. represent an upper limit for real, lab-synthesized QD films. Since, to the best of our knowledge, there are no experimental characterizations of the transport properties of GaSb QD films, with this theoretical study, we provide the first insights into the transport properties of this material.

STOICHIOMETRY EFFECT

Together with the material, the stoichiometry of the QDs is also a vital parameter to take into consideration. We calculated the transport properties of InAs QD films (we chose the material with the highest mobility) using impurity dots with the same number of atoms but with inverted stoichiometry (and thus, an anion-rich surface like the periodic dots). In this case, we find that the resulting mobility at room temperature is increased from ~0.85 to ~1.42 cm^2 V^{-1} s^{-1} for a separation of 1 b.l., as shown in Figs. S7 and S8 (supplementary material).

The mobility for this system is comparable with that observed in $CsPbBr_3$ perovskite QD films[34] (2 cm^2 V^{-1} s^{-1}) and an order of magnitude higher compared to conventional PbS and PbSe QD films.[21] This can be attributed to the increased overlap between the wave functions of neighboring dots and to the longer flight times of the carriers that determine the mobility. Indeed, as there is no effect of the impurity dot on the miniband structure in first order perturbation theory, the resulting minibands for this case are the same as in the case of InAs QD films with anion-rich periodic dots and cation-rich impurities. Consequently, we find that the increase in mobility obtained inverting the stoichiometry of the impurity dot is due to an increase in the flight times, as shown in Fig. 5 (where the miniband width is also shown for each material, along with the corresponding flight times for d = 1 b.l.). The resulting mobility is higher compared to the CdSe (zb) QD films that were modeled previously.[6,13,35,36]

The relation between this width and the interdot separation is illustrated in the inset of Fig. S10, where we show that as the interdot separation is increased, the miniband width is reduced due to the decrease in the wave function overlaps. In our case, the mobility and the miniband width both have a decay trend with increasing interdot separation. The deviation from the expected trend in the width at the lowest separation for InP and InSb is due to the nature of their miniband structure (see Fig. 1), where the lowermost miniband is very close to the second conduction eigenstate. As a consequence, the lowest conduction miniband reaches the lower point in energy of the following miniband, which blocks the expected expansion of the lowermost miniband width.

In order to provide a more quantitative estimate of the mobility dependence on temperature and interdot separation, we fitted our results with a power law $\mu = A + Bx^n$ (where $x = T, d$). Table S2 (supplementary material) contains all the parameter values extracted

from the fit to our temperature-dependent results. Parameter n indicates how the temperature affects the mobility. Depending on the interdot separation, we find two separate behaviors: $n > 0$ for dense dot arrays and $n < 0$ for $d \sim 2$ b.l. Parameter A shows the mobility value at $T = 0$ K (for $n > 0$) and T $\approx \infty$ (for $n < 0$). Parameter B is found to always have the opposite sign compared to n. For $n > 0$, the higher the value of B (negative value), the larger the variation of mobility with increasing T. For $n < 0$, the higher the value of B (positive), the smoother the variation is.

The temperature effect on the mobility is an important parameter for devices, as higher operating temperatures lead to a significant reduction in mobility. Consequently, the goal is to find materials that combine high mobilities and a "resilient" behavior to high operating temperatures. We predict that InP QD films should exhibit the slowest mobility reduction rate with increasing temperature at the smallest separation, as shown in Fig. 6. Although we find that n, in this case, has the largest (more positive) value compared to the other materials, meaning that the mobility (μ) should be affected most with increasing temperature (since $\mu \propto T^n$), this is not the case as the value of B is the smallest leading to the conclusion that the decay rate is the slowest. The value of n becomes negative at $d = 1.9$ b.l. for all In-based QD films considered here, meaning that as the QDs in the array are placed even further apart, the mobility is reduced at a higher rate. On the other hand, the behavior of GaSb QD films is different: even though the decay rate is the fastest at the smallest separation, as d is increased, the mobility is affected less with increasing temperature compared to the In-based materials. Specifically, at $d = 1.9$ b.l., GaSb is the only material to keep a positive value for n. This indicates that for GaSb QD films, even though the lowest mobility is predicted, a smaller mobility reduction rate for $1 < d < 2.2$ b.l. is found.

To investigate the effect of interdot separation, we used a similar expression $\mu = C/d^m$. The values of the extracted fitting parameters are shown in Table S3 (supplementary material). Parameters C and m have a similar effect to B and n in the previous analysis: the larger their value, the larger the dependence of the mobility to increasing d. We find that at $T = 70$ K as m has the lowest value, InP QD films are the least affected by the increase in d, as shown in Fig. 7. In addition, the value of C is the smallest among the In-based materials, suggesting that InP QD films would perform well at low operating temperatures, being less sensitive to the interdot separation, which, in realistic systems, could easily exceed 1 b.l. On the other hand, GaSb QD films exhibit the best behavior at higher temperatures (300 K). Finally, of all materials considered here, InAs QD films are influenced the most by the increase in d at both temperatures.

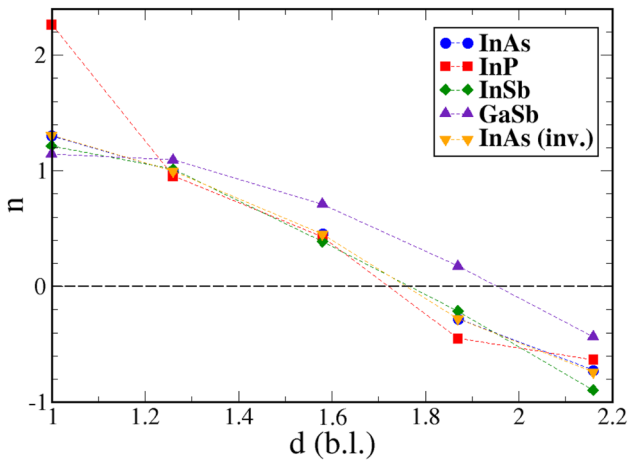

FIG. 6. Rate of mobility reduction with increasing temperature (n) vs d according to the fitting of $\mu = A + BT^n$.

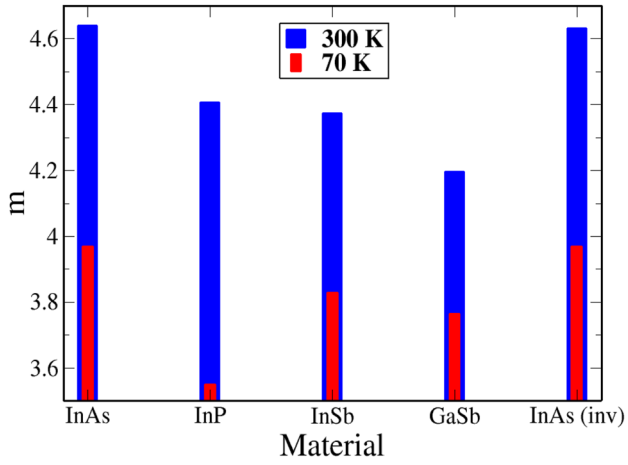

FIG. 7. Rate of mobility reduction with increasing d (m) at $T = 70$ K (red) and 300 K (blue), for each material according to the fitting of $\mu = C/d^m$.

CONCLUSIONS

We calculated the transport properties of promising "green" QD films for replacing their currently used toxic counterparts (e.g., CdSe, PbSe, PbS) in realistic QD films, following a tight-binding model based on an atomistic approach. We find that (i) as the temperature of the film is increased, the mobility decreases, (ii) this reduction rate changes from ~ linear ($n > 0$) to ~ T^n ($n < 0$) as the interdot separation is increased, and (iii) the mobility for a specific temperature is reduced as the separation is increased due to the decreased overlap between the electron wave functions, resulting in reduced miniband widths, flight times, and, thus, mobility values. This is predicted for all materials considered here.

We predict that InAs films exhibit the highest mobility among the rest of In-based QDs, even higher compared to predictions for zb CdSe and to experimental Pb-based systems, making InAs QD films an ideal heavy-metal-free alternative. We see that replacing As with Sb and then with P leads to small changes in the mobility, while replacing In with Ga results in a significant decrease in the mobility. Specifically, we show that the mobilities of ideally passivated InP QD films could be an order of magnitude larger compared to experiment (where the problematic passivation of real InP QDs prevents efficient transport). A quantitative investigation was carried out by applying a theoretical fitting to our results showing that InP QD films are the most resilient to increasing temperature at $d = 1$ b.l. and to increasing d at $T = 70$ K. We conclude that InP QD films

can be a good candidate for replacing currently used toxic materials such as PbS. We also show that the mobility of GaSb QD films is about three times smaller compared to InSb films, even though they have larger miniband width with increasing interdot separation. This is attributed to the smallest flight times (almost four times smaller compared to InSb). Additionally, the two eigenvalues of the mobility tensor calculated for this material are very close in contrast with the other materials due to the isotropic nature of the lowermost miniband, while an anisotropic formation of the miniband structure leads to a larger difference between the mobility eigenvalues. This could affect the performance of realistic systems as an isotropic miniband would imply smaller difference between the two mobility eigenvalues, meaning that no matter in what direction the contacts are placed on the film, the observed mobility would be approximately the same. An anisotropic miniband would lead to a larger difference between the mobility eigenvalues. As a result, the measured mobilities would depend on the direction along the film at which the contacts are positioned. Finally, inverting the stoichiometry of the impurity dot in InAs films leads to a significant increase in the carrier flight times and, thus, mobility, leading to the conclusion that the stoichiometry plays an important role in band-like transport as it can lead to a dramatic increase in both the wave function overlap between the QDs in the array and the flight times. This suggests that a QD film made of QDs with a similar surface composition could yield higher mobilities. Our findings were compared with the available experimental data showing good qualitative agreement with the trend of mobility reduction with increasing temperature for InAs QDs films, while in the other cases (InSb, InP, and GaSb), we provide the first insights into the band-like transport in QD films made of these materials.

SUPPLEMENTARY MATERIAL

See the supplementary material for the mobility calculations for the rest of the materials considered here. The lowermost conduction miniband visualization in the reciprocal space is also included, along with the tables of flight times and fitting parameters.

ACKNOWLEDGMENTS

This work was undertaken on ARC3, part of the High Performance Computing Facilities at the University of Leeds, UK. P.R. gratefully acknowledges financial support from EPSRC through a Doctoral Training Grant. F.M.G.C., S.R.B., and E.S.S.-G. received financial support from Project No. P18-RT-3303 from the Spanish Junta de Andalucia. M.C. is thankful to the School of Electronic and Electrical Engineering, University of Leeds, for financial support.

AUTHOR DECLARATIONS

Conflict of Interest

The authors have no conflicts of interest to declare.

DATA AVAILABILITY

The data that support the findings of this study are available within the article and its supplementary material.

REFERENCES

[1] D. V. Talapin, J.-S. Lee, M. V. Kovalenko, and E. V. Shevchenko, Chem. Rev. **110**, 389–458 (2010).
[2] M. V. Kovalenko, L. Manna, A. Cabot, Z. Hens, D. V. Talapin, C. R. Kagan, V. I. Klimov, A. L. Rogach, P. Reiss, D. J. Milliron, P. Guyot-Sionnnest, G. Konstantatos, W. J. Parak, T. Hyeon, B. A. Korgel, C. B. Murray, and W. Heiss, ACS Nano **9**, 1012–1057 (2015).
[3] J.-H. Choi, A. T. Fafarman, S. J. Oh, D. K. Ko, D. K. Kim, B. T. Diroll, S. Muramoto, J. G. Gillen, and C. B. Murray, Nano Lett. **12**, 2631–2638 (2013).
[4] D. Yu, C. Wang, B. L. Wehrenberg, and P. Guyot-Sionnest, Phys. Rev. Lett. **92**, 216802 (2004).
[5] X. Lan, M. Chen, M. H. Hudson, V. Kamysbayev, Y. Wang, P. Guyot-Sionnest, and D. V. Talapin, J. Mater. Chem. C **19**, 323–329 (2020).
[6] F. M. Gómez-Campos, S. Rodríguez-Bolívar, E. S. Skibinsky-Gitlin, and M. Califano, Nanoscale **10**, 9679 (2018).
[7] C. Buurma, R. E. Pimpinella, A. J. Ciani, J. S. Feldman, C. H. Grein, and P. Guyot-Sionnest, Proc. SPIE **9933**, 993303 (2016).
[8] L. Hu, S. Huang, R. Patterson, and J. E. Halpert, J. Mater. Chem. C **7**, 4497–4502 (2019).
[9] R. Liang, D. Yan, R. Tian, X. Yu, W. Shi, C. Li, M. Wei, D. G. Evans, and X. Duan, Chem. Mater. **26**, 2595–2600 (2014).
[10] T. Kim, S. Lim, S. Yun, S. Jeong, T. Park, and J. Choi, Small **16**, 2002460 (2020).
[11] D. V. Talapin and C. B. Murray, Science **310**, 86–89 (2005).
[12] G. Xu, S. Zeng, B. Zhang, M. T. Swihart, K.-T. Yong, and P. N. Prasad, Chem. Rev. **116**, 12234–12327 (2016).
[13] F. M. Gómez-Campos, S. Rodríguez-Bolívar, and M. Califano, ACS Photonics **3**, 2059–2067 (2016).
[14] A. Shabaev, A. L. Efros, and A. L. Efros, Nano Lett. **13**, 5454–5461 (2013).
[15] P. A. Graf, K. Kim, W. B. Jones, and L.-W. Wang, J. Comput. Phys. **224**, 824–835 (2007).
[16] L.-W. Wang and A. Zunger, Phys. Rev. B **51**, 17398–17416 (1995).
[17] J.-S. Lee, M. V. Kovalenko, J. Huang, D. S. Chung, and D. V. Talapin, Nat. Nanotechnol. **6**, 348–352 (2011).
[18] D. A. Mirabella, C. M. Aldao, and R. R. Deza, Int. J. Quantum Chem. **68**, 285–291 (1998).
[19] W. Liu, J.-S. Lee, and D. V. Talapin, J. Am. Chem. Soc. **135**, 1349–1357 (2013).
[20] A. Okamoto, H. Geka, I. Shibasaki, and K. Yoshida, J. Cryst. Growth **278**, 604–609 (2005).
[21] E. M. Sanehira, A. R. Marshall, J. A. Christians, S. P. Harvey, P. N. Ciesielski, L. M. Wheeler, P. Schulz, L. Y. Lin, M. C. Beard, and J. M. Luther, Sci. Adv. **3**, eaao4204 (2017).
[22] P. Guyot-Sionnest, J. Phys. Chem. Lett. **3**, 1169–1175 (2012).
[23] Z. Yu, J. Li, D. B. O'Connor, L.-W. Wang, and P. F. Barbara, J. Phys. Chem. B **107**, 5670–5674 (2003).
[24] R. W. Crisp, N. Kirkwood, G. Grimaldi, S. Kinge, L. D. A. Siebbeles, and A. J. Houtepen, ACS Appl. Energy Mater. **1**, 6569–6576 (2018).
[25] R. W. Crisp, R. Callahan, O. G. Reid, D. S. Dolzhnikov, D. V. Talapin, G. Rumbles, J. M. Luther, and N. Kopidakis, J. Phys. Chem. Lett. **6**, 4815–4821 (2015).
[26] T. Zhao, E. D. Goodwin, J. Guo, H. Wang, B. T. Diroll, C. B. Murray, and C. R. Kagan, ACS Nano **10**, 9267–9273 (2016).
[27] G. Grimaldi, R. W. Crisp, S. ten Brinck, F. Zapata, M. van Ouwendorp, N. Renaud, N. Kirkwood, W. H. Evers, S. Kinge, I. Infante, L. D. A. Siebbeles, and A. J. Houtepen, Nat. Commun. **9**, 2310 (2018).
[28] P. Rodosthenous, F. M. Gómez-Campos, and M. Califano, J. Phys. Chem. Lett. **11**, 10124–10130 (2020).
[29] R. W. Crisp, F. S. M. Hashemi, J. Alkemade, N. Kirkwood, G. Grimaldi, S. Kinge, L. D. A. Siebbeles, J. R. van Ommen, and A. J. Houtepen, Adv. Mater. Interfaces **7**, 1901600 (2020).

[30]S. Busatto, M. de Ruiter, J. T. B. H. Jastrzebski, W. Albrecht, V. Pinchetti, S. Brovelli, S. Bals, M.-E. Moret, and C. de Mello Donega, ACS Nano **14**, 13146–13160 (2020).
[31]These results correct our previously published mobilities for InSb,[13] which were mistakenly calculated for an interdot separation larger than 1 b.l.
[32]M. Califano and P. Rodosthenous, ACS Appl. Mater. Interfaces **3**, 4643 (2019).
[33]M. Winslow, S. H. Kodati, S. Lee *et al.*, J. Electron. Mater. **50**, 7293–7302 (2021).
[34]B. Yu, C. Zhang, L. Chen, Z. Qin, X. Huang, X. Wang, and M. Xiao, Nanophotonics **10**, 1943 (2021).
[35]F. M. Gomez-Campos, S. Rodríguez-Bolívar, and M. Califano, J. Nanomater. **2019**, 5106909.
[36]E. S. Skibinsky-Gitlin, S. Rodríguez-Bolívar, M. Califano, and F. M. Gómez-Campos, Phys. Chem. Chem. Phys. **21**, 25872 (2019).